Dynamics of microphytobenthos photosynthetic activity along a depth transect in the sandy northeastern Gulf of Mexico shelf

Michael Santema[1] and Markus Huettel[1*]

[1] Department of Earth, Ocean and Atmospheric Science, Florida State University, 117 N Woodward Ave., Tallahassee, Florida 32306-4320, USA, email: mls08c@my.fsu.edu

Corresponding author, email: mhuettel@fsu.edu

Keywords: Microphytobenthos; primary production; oxygen flux; sandy sediment; West Florida Shelf

Abstract

The temporal and spatial dynamics of microphytobenthos activity in sandy shelf sediments are poorly understood, which limits assessments of the role of the benthic production in the coastal carbon cycle. The goal of this two-year time series study in the northeastern Gulf of Mexico therefore was to determine how benthic primary production rates in the West Florida Shelf change over the seasons and water depth. The study took place in the Big Bend region and used three stations along a transect starting at 5 m water depth and ending 29 km offshore, at 18 m water depth. Multisensor YSI 6600 probes installed at each station recorded key environmental parameters at the seafloor. Sediment cores, collected by SCUBA divers from each of the 3 stations at near-monthly intervals over a two-year time period were incubated in the laboratory for production and consumption rate measurements. Incubation of the cores at 200 $\mu E\ m^{-2}\ s^{-1}$ allowed comparison of potential productivity between stations and seasons. Community light response curves, produced from sediment incubations at different light intensities, were used to calculate benthic productivity for measured in-situ light levels. The benthic production rates calculated from the core incubations and those calculated using the community light response curves agreed within a factor of three. Average sediment gross primary production rates based on in-situ light intensities ranged from 48 ± 60 mg C $m^{-2}\ d^{-1}$ at 5 m and 81 ± 104 mg C $m^{-2}\ d^{-1}$ at 10 m, to 13 ± 18 mg C $m^{-2}\ d^{-1}$ at 18 m water depth. The corresponding average sediment consumption rates were -62 ± 36, -50 ± 55, and -29 ± 46 mg C $m^{-2}\ d^{-1}$ at 5, 10 and 18 m water depth respectively. On average, production and consumption in the benthic system were found to be balanced, and the nearshore Stations A and B may temporarily turn net autotrophic during periods of high light intensity at the bottom. Our results suggest that the benthic production in this region may contribute up to 50% to the shelf primary production.

1. Introduction

Microphytobenthos, a community of microscopic primary producers including diatoms, dinoflagellates, and cyanobacteria, colonizes the surfaces of marine soft and hard bottoms where light can reach the sea floor (MacIntyre et al., 1996b; Miller et al., 1996). Although estimates suggest that microphytobenthos may contribute as much as 30% (Ní Longphurt et al., 2007) of the oxygen in the overlying water column and globally fix ~500 Mt C $year^{-1}$ (Cahoon, 1999), the microphytobenthos activities and benthic oxygen production and consumption in the NEGOM and West Florida Shelf are poorly understood (Allison et al., 2013; Baustian et al., 2011). In Florida's Big Bend region, the West Florida Shelf is very wide (175 to 275 km) and shallow (~40% < 100 m northeast of 26° N and 88° W). Approximately 90% of the bottom here is covered by unconsolidated sand (Livingston, 1984), of which ~5% are colonized by seagrasses, mainly in the shallow nearshore zone (Yarbro and Carlson, 2013). In the remaining sand area, microphytobenthos organisms are the main primary producers (Okey, 2002; Okey et al., 2004). Because microphytobenthos production may contribute a significant fraction of the total primary production in the shallow shelf as a whole (Colijn and de Jonge, 1984; Gattuso et al., 2006; MacIntyre et al., 1996b), quantitative data are required to understand magnitude as well as spatial and temporal dynamics of the benthic productivity in the West Florida Shelf and its role for the carbon cycling in the coastal Gulf. The primary goal of this study, therefore, was to determine productivity rates of the microphytobenthos in the Big Bend area of the NEGOM, and to investigate key factors that control the productivity changes along a gradient of increasing water depth. Specifically, the following questions were addressed:

1. How do benthic Chlorophyll *a* concentrations change over water depth and time along the coastal depth gradient?

2. How do benthic primary production rates change over the seasons along the transect?
3. How do different light levels affect the benthic oxygen production?

These questions were addressed through a 2-year time series study combining in-situ measurements along a 29 km transect (5 to 18 m water depth) and laboratory measurements.

2. Methods

2.1. Field Site

The study area was located in the Big Bend of the West Florida Shelf (Fig. 1), south of Tallahassee, in Florida's panhandle. The coastal water in this region is influenced by the Apalachicola River that discharges into the Gulf 60 km west of the study area. The average water column salinity here ranges from 33 ± 3 in spring to 34 ± 2 in winter, and the respective water temperatures from 11 ± 2 °C to 31 ± 3 °C. The bottom currents are driven mainly by tidal forces and wave orbital motion (He and Weisberg, 2002). The sediments are composed of fine to medium quartz sands with some shell hash (Table 1).

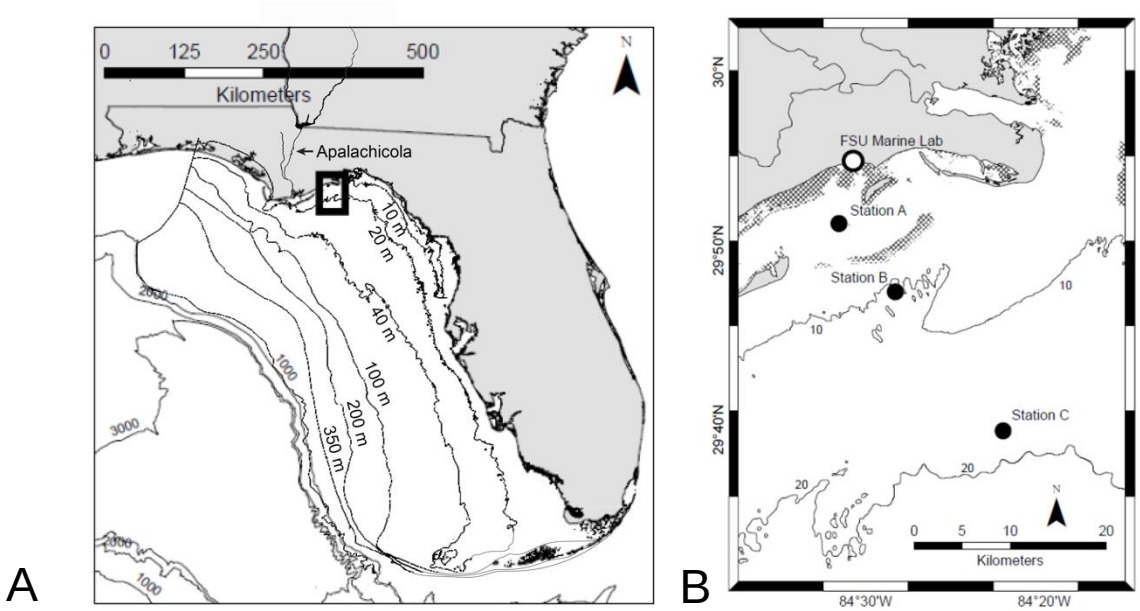

Figure 1. A) Location of the study area (black rectangle). B) Location of the sampling stations A, B and C along the transect where YSI 6600 multi-sensor probes were deployed. Crosshatched regions represent seagrass beds along the coast and on dog island reef (a submerged shallow sand bar located between A and B). All bathymetry contours are labeled in meters. Bathymetry data are from NOAA-NCEI (2017) and seagrass cover data are from NOAA-NOS (2015).

Table 1. Ranges for environmental parameters at the 3 stations. Values for temperature, salinity, turbidity and light represent data recorded at 50 cm above the seafloor. Dissolved inorganic nitrogen (DIN), phosphate (PO_4^{3-}) and silicic acid ($Si(OH)_4$)) concentration ranges were measured in the upper water column (~1 m) except Station C values in parenthesis that represent concentrations measured 0.5 m above seafloor in January 2008. Zero values listed for PO_4^{3-} and $Si(OH)_4$ reflect concentrations that were below detection limit.

		Station		
Parameter	Unit	A	B	C
Latitude		29° 51.50' N	29° 47.67' N	29° 39.90' N
Longitude		84° 31.50' W	84° 28.33' W	84° 22.29' W
Depth	(m)	5	10	18
Temperature	(°C)	11 – 31	11 – 30	17 – 30
Salinity		30 – 37	33 – 37	33 – 36
Current speed	($m\ s^{-1}$)	0 – 4.7	0 – 3.4	0 – 0.5
Turbidity	(NTU)	11.6 ± 16.2	2.9 ± 13.2	1.9 ± 10.1
Light	($PAR\ \mu E\ m^{-2}\ s^{-1}$)	0.4 – 448	1.4 – 317	1 – 267
Sediment type (Sheppard)		Sand	Sand	Sand
Grain size median	median (μm)	269 ±1.8	313 ± 1.7	428 ± 2.1
Permeability	(m^{-2})	2.3×10^{-13} - 6.4×10^{-12}	1.5×10^{-11} - 2.5×10^{-11}	4.4×10^{-12} - 3.3×10^{-11}
DIN	($mmol\ m^{-3}$)	0.02 – 2.48	0.19 – 1.96	0.29 – 2.43 (0.9)
PO_4^{3-}	($mmol\ m^{-3}$)	0 – 0.32	0 – 0.15	0 – 0.17 (0.1)
$Si(OH)_4$	($mmol\ m^{-3}$)	0.07 – 23.28	0 – 11.29	0 – 6.83 (0.3)

2.2. Study transect

The study transect extended in southeast direction from the Florida State University Coastal Marine Laboratory in St. Teresa, Florida, to K-Tower, a retired US Air Force radio tower located 29 km offshore (Fig. 1B). Along this transect, three stations with instrument platforms were established at the seafloor: "Station A", at 5 m depth, "Station B", at 10 m depth, and "Station C" at 18 m depth (Table 1). The freshwater input of the Apalachicola River caused salinity fluctuations that were largest at station A. Warmer Gulf water caused a temperature buffering at the outermost station C during winter (Table 1). Finer, siltier material, imported into our transect near the coast by the Apalachicola River (Livingston, 1984), and increasing shell debris content with increasing distance from shore caused the coarsening of the sandy sediment from station A to station C. At all stations, the upper 20 cm of the sediment were highly permeable ($k > 10^{-12}$ m^2), permitting advective pore water exchange (Huettel et al., 2014). The seafloor at the three stations typically was covered by sand ripples reflecting bedload transport that impeded macrophyte colonization.

Microphytobenthos consisting mainly of pennate diatoms (*Amphora, Navicula, Nitzschia* and others) and cyanobacteria (*Lyngbya, Microcoleus* and others) (Huettel, unpublished) was present at all stations. In this study, we use the functional definition of "microphytobenthos" introduced by MacIntyre et al. (1996) that includes settled phytoplankton. This microphytobenthos was responsible for the benthic photosynthesis measured as oxygen production in this study. The macrofauna (> 1 mm) in the sands was dominated by orbiniid polychaetes (< 500 m^{-2}) and small decapod crustaceans (< 2000 m^{-2}) (Chipman et al., 2012). A survey conducted in the Big Bend area suggests that benthic macrofauna abundances in the sand typically do not exceed 5000 individuals m^{-2} (Posey et al., 1998).

114 2.3. In-situ measurements

115 The study covered the time period June 2008 to September 2010. At the three transect
116 stations, YSI 6600® multi-sensor probes were installed in bottom mounts for measurements of
117 salinity, temperature, pressure, pH, Chlorophyll *a*, dissolved oxygen and PAR. The latter was
118 measured by a Li-Cor® planar PAR sensor pointing straight up. All data were logged at 15 min
119 intervals. Wiper mechanisms kept the sensing surfaces of the oxygen, chlorophyll, and light
120 sensors clean of settling sediment and biofouling. All sensors were measuring at 50 cm above the
121 sea floor, which in the text to follow is referred to as "at the seafloor". The probes were
122 calibrated prior to each deployment according to the manufacturer's guidelines, which were 2-
123 point calibrations with the equations determined internally by the YSI probe. The calibration
124 endpoints for the measured parameters were 0 - 60 mS cm^{-1} (25 °C) for conductivity (later
125 converted to salinity), 0 - 30 °C for temperature, 7 to 10 for pH, 0 to 100 % saturation for O_2
126 saturation, 0 to 123 NTU for turbidity, and 0 to 50 mg Chl *a* m^{-3} for Chlorophyll *a* (dissolved
127 standard). The YSI probe calculates the Chl *a* concentrations from the fluorescence data it
128 collects and the internal calibration curve it generates from the calibration. Pressure and PAR
129 sensors were factory-calibrated, requiring 2-year recalibration intervals. The multi-probes were
130 turned around about once every month for routine cleaning, repair, calibration, and data
131 downloading. Bad weather and biofouling caused several gaps in the data series as instruments
132 either could not be retrieved in time or the instrument failed. As part of a related project, an
133 acoustic Doppler current profiler (ADCP) was installed in the bottom mount at each of the 3
134 stations alongside the YSI® multi-sensor probes. These devices logged horizontal current
135 velocity at distinct horizontal layers evenly spaced throughout the water column. Flow velocities
136 and flow directions 1-2 m above the sea floor at Stations A and B, and 3-4 m above the sea floor

at Station C were averaged over 15 min periods for calculating daily means of bottom flow. The detailed results of these ADCP measurements are reported elsewhere (Maksimova and Clarke, 2013; Mortenson, 2013).

2.4. Sediment and water sampling

Starting in August 2008, 8 cylindrical sediment cores (3.6 cm diameter, 10 cm long) were collected by SCUBA divers from each of the 3 stations at near-monthly intervals for productivity measurements (2008 (m/d): 9/23, 10/10, 11/19, 2009: 1/22, 2/24, 3/10, 3/31, 4/16, 4/23, 5/5, 5/12, 6/9, 6/30, 7/28, 9/3, 10/6, 11/24, 12/14, 2010: 1/20, 1/27, 3/8, 3/24, 4/7, 4/29, 6/26, 7/15, 8/25, 9/3). The number of sediment collections across the different seasons is shown in Table 2.

Table 2: Count of sediment sampling periods by season, site, and year.

Site	Season	Year			Total
		2008	2009	2010	
A	Winter		2	2	4
	Spring		1		1
	Summer		1	2	3
	Fall	3	3		6
B	Winter		1	1	2
	Spring		2	1	3
	Summer			1	1
	Fall	3		1	4
C	Winter		2	2	4
	Spring		3	1	4
	Summer		2	1	3
	Fall	1	1	1	3

There were seasons throughout the study period when collecting cores at certain sites was not feasible, leading to some seasons with more sediment cores than others. The sediment cores were stored immediately after retrieval in coolers at in-situ temperature in the dark and brought to the laboratory within 2 h. Here, 4 cores from each station were placed in an environmental chamber set to in situ temperature for net oxygen production and consumption rate

160 determinations. The remaining cores were placed in a refrigerator to await Chlorophyll *a*
161 analysis. No cores could be collected in summer 2009 and in fall 2009 at Stations B and C due to
162 adverse weather conditions, unavailability of divers, or maintenance of the research vessel.
163 In January 2008, during the period when water column nutrient concentration in this
164 region typically reaches its annual maximum, bottom water samples were collected at Station C
165 by SCUBA divers at 0.5 m above the seafloor for nutrient analysis (dissolved inorganic nitrogen
166 (DIN), phosphate (PO_4^{3-}) and silicic acid ($Si(OH)_4$)) according to Grasshoff et al. (1999). In
167 addition, seasonal surface water samples (~1 m water depth, all stations) were collected from
168 August 2007 to August 2008 and analyzed using the same procedures (Santema et al., 2015).
169
170 2.5. Chlorophyll *a* Analysis
171 The upper 10 cm of the cores collected for Chlorophyll *a* analysis were sectioned at 1 cm
172 depth intervals. The sections were placed into 15 ml centrifuge vials, submerged in 5 ml of
173 buffered 90% acetone, shaken vigorously, and left overnight in a refrigerator for Chlorophyll *a*
174 extraction. The vials then were centrifuged and the supernatant decanted into a quartz cuvette.
175 Chlorophyll *a* content in the sample was measured with a Turner™ Model 10 fluorometer
176 according to the fluorometric method described by Parsons et al. (1984). The sediment section
177 was dried and weighed. Chlorophyll *a* content in the sediment section was calculated and is
178 reported here as Chl *a* g^{-1} dry sediment.
179
180 2.6. Determination of the benthic productivity
181 Two approaches were used to determine and compare the ranges of benthic productivity
182 at the three stations:

1) Measurements of potential production at a specific light intensity. This first approach used laboratory core incubations under light and dark conditions and determined oxygen production and consumption of the incubated sediments. To allow a comparison of potential production between stations and seasons, the same light conditions were applied for all core incubations. 2) Determination of benthic productivity using community light response curves. This second approach used the in-situ light recordings and community light response curves (sediment gross production/light relations) to calculate estimates for in-situ gross production.

2.6.1. Measurements of potential productivity at a specific light intensity

To compare the seasonal potential benthic production and consumption rates, sediment cores from the three stations were incubated under light and dark conditions in an environmental chamber set to in situ temperature. The cores with overlying water column were closed without headspace by a transparent lid. Then the sediment surfaces were subjected over a period of about 24 h to changing light conditions, with 2 h illumination alternating with 2 hours of complete darkness. The light conditions at the seafloor at the three stations were highly variable but the ranges of the light intensities at the three stations were similar as the increasing turbidity toward the coast offset the effect of the decreasing water depth. To allow the comparison of the potential benthic productivity between the three stations and between seasons, the same photosynthetically active radiation (PAR) of 200 µE m^{-2} s^{-1} was applied by a Xenon lamp in all incubations. This light intensity was within the natural range of light intensities experienced by the microphytobenthos at the three stations (maximum in-situ light intensities recorded at the three stations A: 28 May 2008, 448 µE m^{-2} s^{-1}, B: 7 Aug 2010, 317 µE m^{-2} s^{-1}, C: 12 Apr 2008, 267 µE m^{-2} s^{-1}). The 2 h measuring periods were chosen to avoid oxygen-oversaturation of the water

206 overlying the sediment and to minimize effects caused by changes occurring in the cores over
207 time. The water overlying the cores, filtered through GFF filters, was circulated with a Rainin®
208 Dynamax RP-1 peristaltic pump through a closed loop of gas-tight black Tygon® tubing. Flow
209 over the sediment surface was adjusted to correspond to a realistic bottom water current u of $1 <$
210 $u < 3$ cm s^{-1}. An optode sensor, integrated in the recirculation loop, measured dissolved-oxygen
211 in the water overlying the sediment, which was used as proxy for carbon fixation and carbon
212 mineralization (Canfield et al., 1993). For all sediment incubations up to September 2009, the
213 oxygen sensor was a Presens™ fiber optic flow-through sensor attached to a Presens™ Microx
214 TX3 oxygen meter, after that, a Hach® LDO101 rugged optical oxygen probe mounted in a
215 custom-made flow through cell and attached to a Hach® HQ40d multi-meter was used. Presens
216 and Hach optodes were calibrated according to manufacturer instructions using air saturated
217 water (air-bubbled water) and oxygen-free water (purging with N_2 for over 10 minutes). Gross
218 production rates were calculated by subtracting consumption rates (negative values) measured
219 during dark periods from net production rates measured during light periods.
220
221 2.6.2. Determination of benthic productivity using community light response curves.
222 To assess the relationship between sedimentary primary production and light intensity,
223 and to determine the potential daily sedimentary photosynthetic production at the three stations,
224 oxygen production of the sediments was measured for the natural range of light intensities. For
225 the measurement of these community light response curves, sediment cores were collected from
226 each of the 3 stations in July 2011. The cores were returned to the lab and kept at in situ
227 temperature. The sediment of the top 1 cm of a 3.6 cm diameter sediment core was removed and
228 spread out evenly onto the bottom of a gas-tight cylindrical chamber (19 cm diameter, 2 cm

height), thereby producing a sediment layer of approximately 1 grain-diameter thickness (~0.3 mm). Through this thin-layer-approach, all algae associated with the sand received light and the sediment was kept fully oxic. The chamber then was filled with artificial seawater (Instant Ocean™, S = 35, PO_4^{3-}: 0.05 µmol l^{-1}, NO_3^-: 1 µmol l^{-1}, NH_4^+: 10.2 µmol l^{-1}, $Si(OH)_4$: 4.2 µmol l^{-1}) and sealed bubble-free with a sheet of clear glass. Oxygen inside the chamber was recorded with a Presens™ optode, inserted through a port in the sidewall of the chamber. The chamber was maintained at in situ temperature by placing it inside a shallow water bath controlled by a cooling unit, with the upper surface of the chamber remaining above the water level of the bath. A Onset HOBO temperature logger in the bath monitored the temperature. To keep oxygen distribution inside the chamber homogenous, the chamber water was gently stirred with a magnetic stir bar. This experimental setup was placed outside during three sunny days, where the sediments were exposed to natural sunlight. Light intensities ranging from 0 to 1200 µE m^{-2} s^{-1} (Fig. 2) were applied to the sediment by placing different numbers of frames with black window screen into the light path. Light intensity below the screens was constantly logged with a Li-Cor® spherical PAR sensor attached to a Li-Cor® LI-1400 data logger. Shades were adjusted to achieve light intensities close to 25, 50, 75, 100, 250, 500, 750, and 1000 µE m^{-2} s^{-1}. Target light intensities were spaced to allow calculation of the expected logarithmic Photosynthesis-Irradiation relationship (MacIntyre, 2002). Periods of light and dark were measured in three replicates at each light intensity, yielding 24 total light-dark pairs measured. For each light intensity, 3 periods of 10 minutes of illumination were recorded. The illumination periods were separated by 10 minutes of complete darkness, achieved by covering the entire system with an opaque tarp. This permitted comparing rates of light net oxygen production to rates of dark oxygen consumption. The resulting O_2 production over PAR relationship was fit to a logarithmic

252 least-squares trend. Outliers falling outside the 95% confidence interval of the regression of all
253 data points (reported in the Supplemental Materials) were excluded from the regressions used for
254 calculating the production rates. The resulting light intensity/gross oxygen production
255 relationships hereafter are referred to as Community Light Response (CLR) curves because they
256 differ from traditional Photosynthesis-Irradiance (P-I) curves (Platt et al., 1980; Walsby, 1997).
257 In contrast to the P-I curve that describes the photosynthetic response of photosynthesizing
258 organisms to different light intensities, our CLR curves describe rates that reflect the response of
259 complex sedimentary communities. The latter were comprised of many different species of
260 autotrophs but also included a large variety of heterotrophs (e.g., bacteria, meiofauna) and
261 geochemical processes (e.g., iron oxidation) that occur naturally in marine sediments and
262 consume oxygen under light and dark conditions.

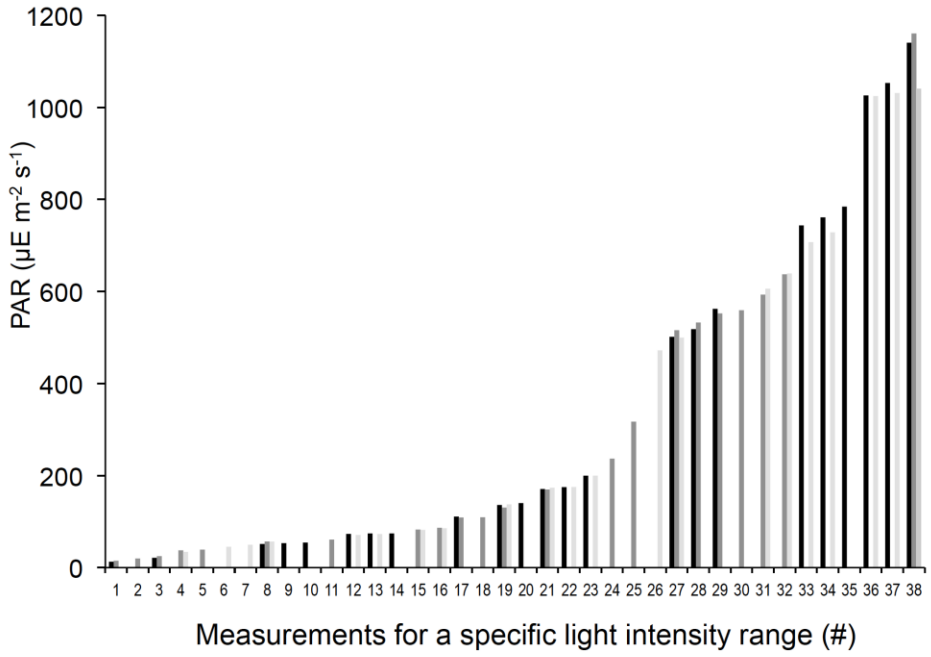

263

264 **Figure 2:** Light intensity ranges applied to the surface sediments of station A (black columns),
265 B (dark grey columns) and C (light grey columns). A total of 38 light intensity ranges were
266 applied. Because the illumination was achieved by manipulating natural sunlight, not all light
267 intensity ranges could be applied to all stations equally.

2.7. Statistical Treatment

Student's t-tests were performed to compare Chlorophyll *a* concentrations and gross oxygen production and consumption rates from the sediment between the different stations. All data appeared normally distributed on histograms, and the appropriate t-test was run depending on homoscedasticity from F-test results. Total Chlorophyll *a* measurements were compared between stations as well as measurements done for each depth layer of the sediment. Two-way ANOVAs were used to test differences between stations and seasons. For gross oxygen production and consumption, all rates over all seasons were compared. The astronomical ending dates of seasons (solstice or equinox) were used to assign data to seasons. The lengths of the daily average seasonal light and dark periods were calculated from published (http://aa.usno.navy.mil) sunrise and sunset data (Winter: 10.95 h light, 13.05 h dark, Spring: 13.30 h, 10.70 h, Summer: 13.34 h, 10.66 h, Fall: 10.99 h, 13.01 h) and were used to convert hourly to daily rates. Where error margins are listed, the error value represents one standard deviation. The conversion from oxygen to carbon equivalents used a respiratory quotient of 1.3 (Allesson et al., 2016).

To evaluate influences of bottom water characteristics on the benthic primary productivity, a Principal Component Analysis (PCA) was performed on the continuously recorded environmental data, including variables measured by the YSI multi-probes (bottom water dissolved O_2, Chl *a*, temperature and salinity), Panacea NCDC station weather data (surface PAR), and Apalachicola River discharge recorded at the USGS Sumatra station (USGS, 2011). Other metrics like turbidity, bottom PAR, and pH were too intermittent to be included in the model. The PCA included data from all sites. All data were standardized ($\frac{x-\mu}{\sigma}$ where μ is mean and σ is standard deviation) and normalized (logarithm base 10 of logarithmically

291 distributed data: Chl *a* and river discharge). Sediment O_2 production data (Section 3.2.) for each
292 of the 3 sites were divided equally in half into two groups with low and high production,
293 respectively. The dates the sediment samples were collected were chosen as the scores of the
294 PCA to observe how production was related to the different environmental variables.
295
296 **3. Results**
297
298 Mean daily maximum PAR intensities at the water surface ranged from 1353 ± 303 µmol
299 m^{-2} s^{-1} in winter to 1906 ± 314 µmol m^{-2} s^{-1} in summer (Fig. 3). The seafloor along the transect
300 year-round received sufficient light for benthic photosynthesis, with maximum PAR fluxes
301 reaching 447 µE m^{-2} s^{-1} in spring at Station A. In general, PAR fluxes at the seafloor were
302 highest in spring and summer and lower in fall and winter. PAR fluxes at Station B in winter
303 stand out as the highest values in the set, however, only 10 days of winter PAR data (10-20 Mar
304 2009) could be collected at this station during a fair-weather period when water at B was
305 relatively clear and surface PAR was high. In spring and summer, mean PAR flux recorded at the
306 seafloor at the shallowest station (A) exceeded those measured at Stations B and C, while in fall
307 and winter, light fluxes at Station A were similar to those at C. The seasonal variability of light at
308 the seafloor increased with the seasonal increase of light intensity at the water surface.
309

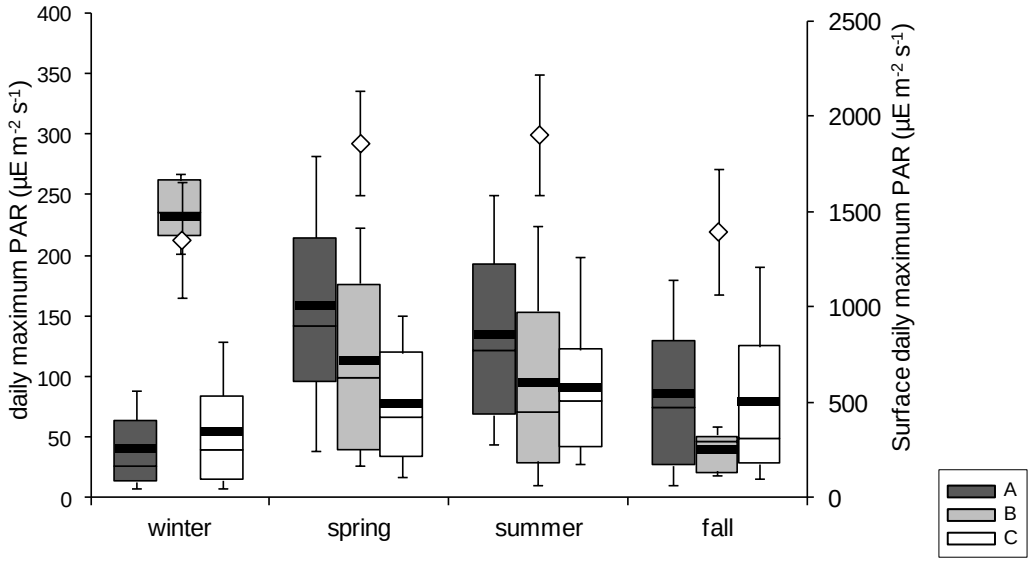

Figure 3. Ranges of light for the four seasons at three stations: A, B, and C. Winter PAR fluxes at station B may not be representative due to limited data availability. In the gray boxes, heavy lines depict means and thin lines are medians. Box highest and lowest values are the 25th and 75th percentiles, and whiskers are the 10th and 90th percentiles. White diamonds represent light intensity at the water surface, using the secondary y-axis on the right. Error bars for the diamonds are standard deviation.

3.1. Sediment Chlorophyll *a*

Chlorophyll *a* concentrations in the top 10 cm of sediment ranged from 0.003 µg g^{-1} sed dw (at 9.5 cm depth at Station C, 15 Sep 2010) to 0.502 µg g^{-1} sed dw (at 5.5 cm at A, 24 Feb 2009) and in general were higher at A than at C (t-test $p<0.05$) (Fig. 4). Chl *a* at B was not significantly higher than at C (t-test, $p<0.08$) due to higher variability. Overall Chl *a* concentration means at the three stations were 0.18 ± 0.10 µg g^{-1} sed dw (Station A), 0.19 ± 0.14 µg g^{-1} sed dw (B), 0.11 ± 0.06 µg g^{-1} sed dw (C). Average Chl *a* concentrations were not significantly different between seasons at the same site due to the relatively high variability in the concentrations.

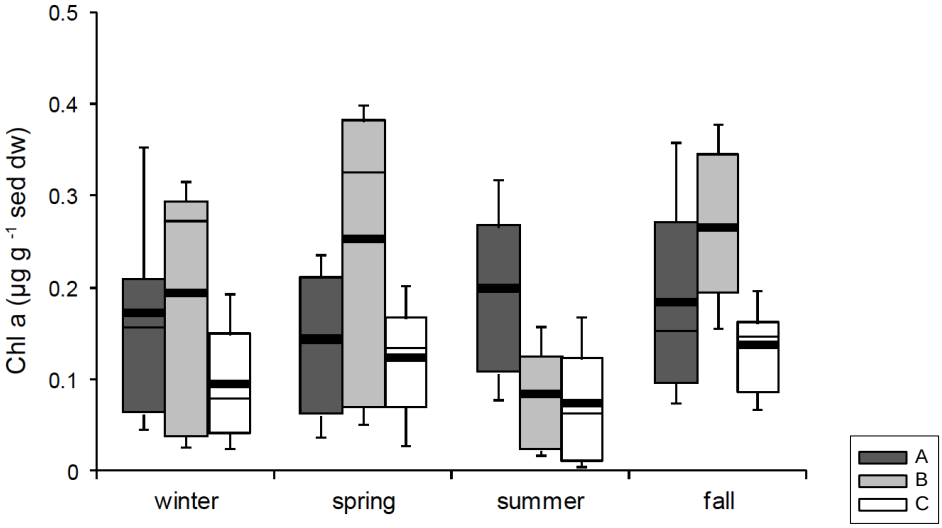

Figure 4. Seasonal ranges of Chlorophyll *a* concentration in the top 10 cm of sediment from the field site. Thick lines are means, thin lines medians, the boxes delineate the 25th and 75th percentiles, and whiskers the 10th and 90th percentiles.

The shapes of the Chl *a* profiles in the upper 10 cm of the sediment differed between seasons and stations. During winter and spring, Chl *a* concentrations at Station A increased from the sediment surface to 4-5 cm depth and then decreased below (Fig. 5). In spring, Chl *a* concentrations at B reached the highest average concentrations recorded during the annual cycle (0.36 ± 0.03 µg g^{-1} sed dw). In summer and fall, the Chl *a* concentrations at all stations were similar with relatively constant concentrations within the upper 5 cm of the sediment, below that layer, the concentrations at station C was lower than at A and B. This was also reflected in the mean annual profiles, in which the average Chl *a* concentrations remained relatively constant over the upper 5-6 cm of the sediment and differed not significantly between stations. Below that layer, concentrations decreased, and at Station C were significantly lower than those recorded at A and B (t-test, $p<0.05$).

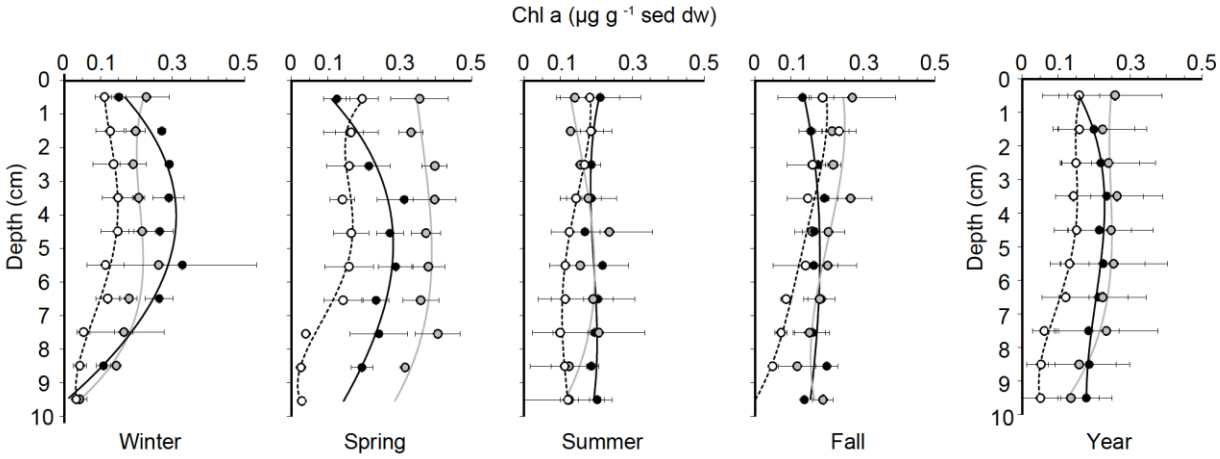

Figure 5. Depth distribution of Chl *a* of all data recorded at Stations A (black circles, black line), B (gray circles, gray line), and C (white circles, dotted line) for the four seasons and the annual average. Error bars represent standard deviation. The lines are third-order polynomial fits.

During the 2-year time series, surface layer Chl *a* (average upper 3 cm), reached highest concentrations in the fall of 2008 with continuing high concentrations until a second peak in May/June 2009. Afterwards, Chl *a* concentrations decreased and remained relatively low until the end of the study period (August 2010). The fall and spring peaks observed in 2008-2009 were also observed in 2009-2010 but were less pronounced (Fig. 6).

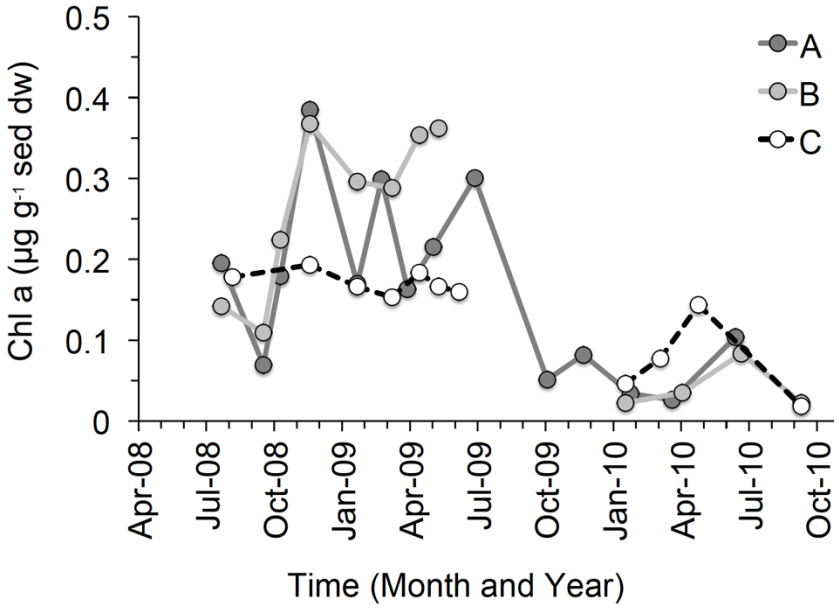

Figure 6. Time course of mean Chlorophyll *a* concentrations in the top 3 cm of sediment as measured from discrete samples in the laboratory over time from the 3 stations.

3.2. Productivity measurements

3.2.1. Laboratory potential productivity measurements

The average potential gross oxygen production measured at an illumination of 200 µE m^{-2} s^{-1} ranged from 0.19 ± 0.06 mmol m^{-2} h^{-1} at Station C in winter to 1.87 ± 0.41 mmol m^{-2} h^{-1} at A in spring, and consumption rates from –0.23 ± 0.16 mmol m^{-2} h^{-1} at C in winter to -0.86 ± 0.19 mmol m^{-2} h^{-1} at A in spring (Fig.7, Table 3). The average gross oxygen production and consumption rates at Station C were significantly lower (t-test, $p<0.05$) than the respective rates

366 calculated for the other 2 stations, and rates at A and B were not significantly different from each
367 other. The seasonal means were statistically different (ANOVA, $F(3,24) = 6.25$, $p < 0.005$) and
368 indicated a trend with highest potential gross production rates in spring, followed by summer and
369 fall, and lowest rates in winter. Consumption rates mirrored the gross production trends, with
370 highest rates in spring and lowest rates in winter. There were exceptions to these trends, most
371 notably at Station B in summer, when potential production and consumption were higher than in
372 spring. The average consumption rates were significantly different between the three stations
373 (ANOVA, $F(2,24) = 9.74$, $p<0.001$) but not between seasons (ANOVA, $F(3,24) = 1.39$, $p>0.05$).
374 The ratio of potential gross oxygen production to consumption was higher at A (1.7 ± 0.5) and B
375 (1.9 ± 1.1) compared to C (C: 1.2 ± 0.4). The potential gross primary production decreased with
376 water depth at rates of -0.034 (winter), -0.115 (spring), -0.030 (summer), -0.024 (fall) mmol m^{-2}
377 h^{-1} m^{-1} (year average -0.051 mmol m^{-2} h^{-1} m^{-1}). The respective rates for sediment oxygen
378 consumption decrease with water depth were 0.015 (winter), 0.044 (spring), 0.012 (summer),
379 0.022 (fall) mmol m^{-2} h^{-1} m^{-1} (year average 0.023 mmol m^{-2} h^{-1} m^{-1}).
380

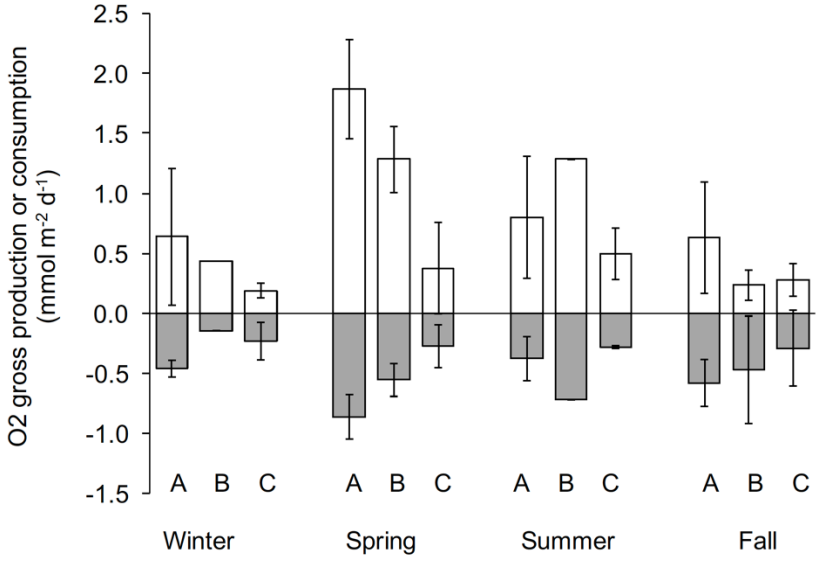

381

Figure 7. Potential gross oxygen production (white columns) and consumption (gray columns) at the 3 stations. Error bars represent standard deviation.

We found no clear correlation between production rates and Chl *a* concentration, but after exclusion of three outliers, higher production was associated with higher Chl *a* concentrations (Fig. 8).

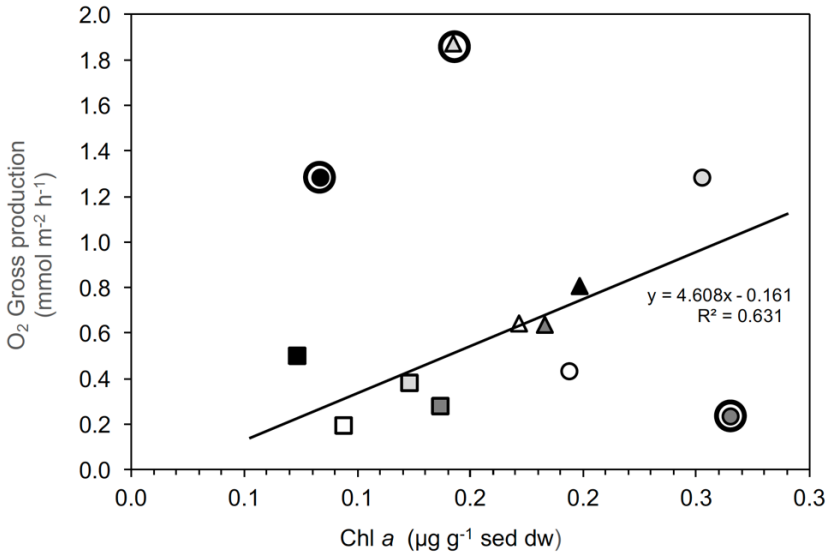

Figure 8: Relationship between O_2 gross production and Chl *a*. The Regression line excludes three outliers marked with circles. White symbols: Winter, light grey symbols: Spring, black symbols: Summer, dark grey symbols: Fall. Triangles: Station A, circles: Station B, Squares: Station C.

3.2.2. Productivity assessments using community light response curves

The exposure of the benthic community to different light levels produced a logarithmic trend typical for photosynthesis-irradiance curves, and revealed the strongest response at Station B, followed by Stations A and C (Fig. 9). This reflected the ranking of benthic Chl *a* measured at the Stations with highest average concentrations at Station B (0.20 ± 0.08 µg g^{-1} sed dw),

400 intermediate at A (0.17 ± 0.02 µg g^{-1} sed dw) and lowest Chl *a* at Station C (0.11 ± 0.03 µg g^{-1}

401 sed dw).

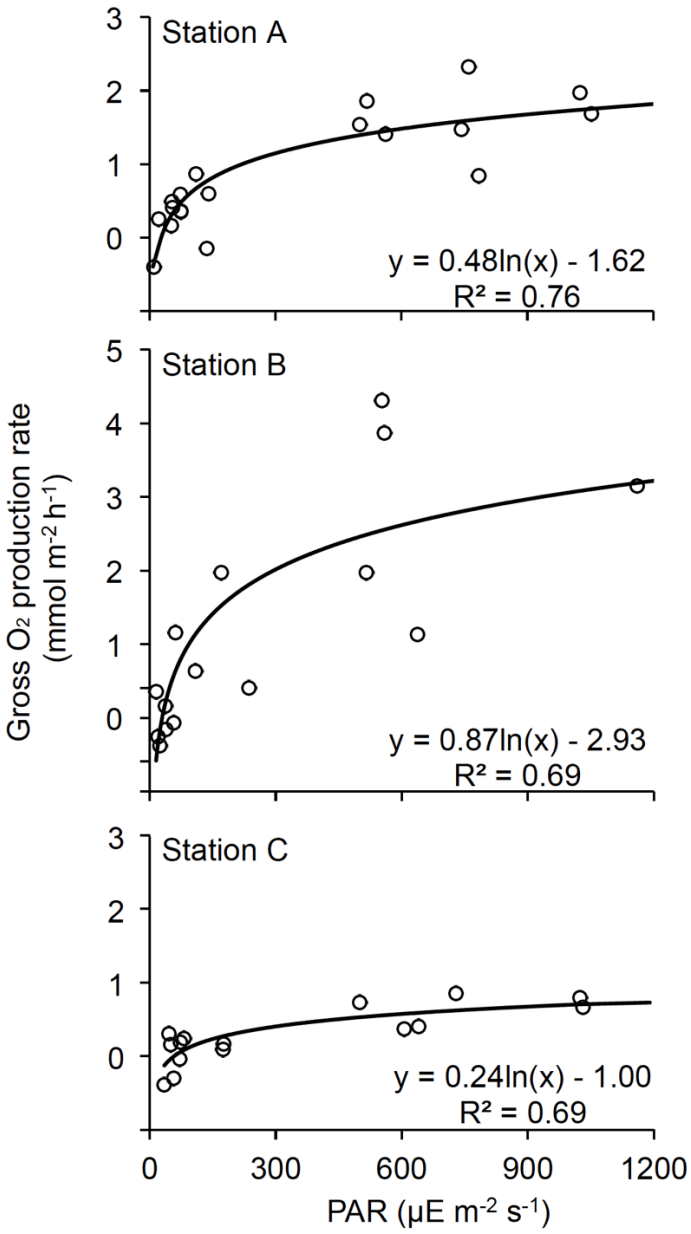

Figure 9. Community light response curves for sediments retrieved from the three stations measured under controlled light conditions by shading natural sunlight. Gas bubble formation or contamination of the oxygen sensor by sediment in some measurements caused artifacts, and data points falling outside the 95% confidence intervals of the response curves calculated from

all data (Supplemental Materials) were excluded from the regression.

Applying the light intensities measured in-situ at the three stations to the respective community light response curves, produced average gross production rates of 0.43 ± 0.52 mmol m^{-2} h^{-1} at Station A, 0.71 ± 0.90 mmol m^{-2} h^{-1} at B, and 0.12 ± 0.16 mmol m^{-2} h^{-1} at C (Fig. 10, Table 3). The average production rates were significantly different between the three stations (ANOVA, $F(2,21) = 31.76$, $p<0.001$) but not between seasons (ANOVA, $F(2,21) = 2.92$, $p>0.05$). Gross primary production decreased with water depth at rates of -0.022, -0.035, -0.034, -0.022 mmol m^{-2} h^{-1} m^{-1} for winter, spring, summer and fall respectively (Fig. 11, year average -0.028 mmol m^{-2} h^{-1} m^{-1}), revealing a 1.6-fold faster decrease with depth during the seasons of high productivity. The average production rates calculated using the in-situ light intensities were factors 2.3 (A), 1.1 (B), and 2.8 (C) lower than the estimates determined at a light intensity of 200 µE m^{-2} s^{-1} in the Laboratory potential productivity measurements (3.2.1., Fig. 10). At this light intensity of 200 µE m^{-2} s^{-1}, the gross production rates calculated using the community light response curves reached 0.95 mmol m^{-2} h^{-1} at Station A, 1.66 mmol m^{-2} h^{-1} at B, and 0.30 mmol m^{-2} h^{-1} at C, and thus were similar to the estimates determined with the Laboratory potential productivity measurements conducted at 200 µE m^{-2} s^{-1} (3.2.1.: A: 0.98 ± 0.98 mmol m^{-2} h^{-1}, B: 0.81 ± 0.30 mmol m^{-2} h^{-1}, C: 0.34 ± 0.46 mmol m^{-2} h^{-1}), except for Station B.

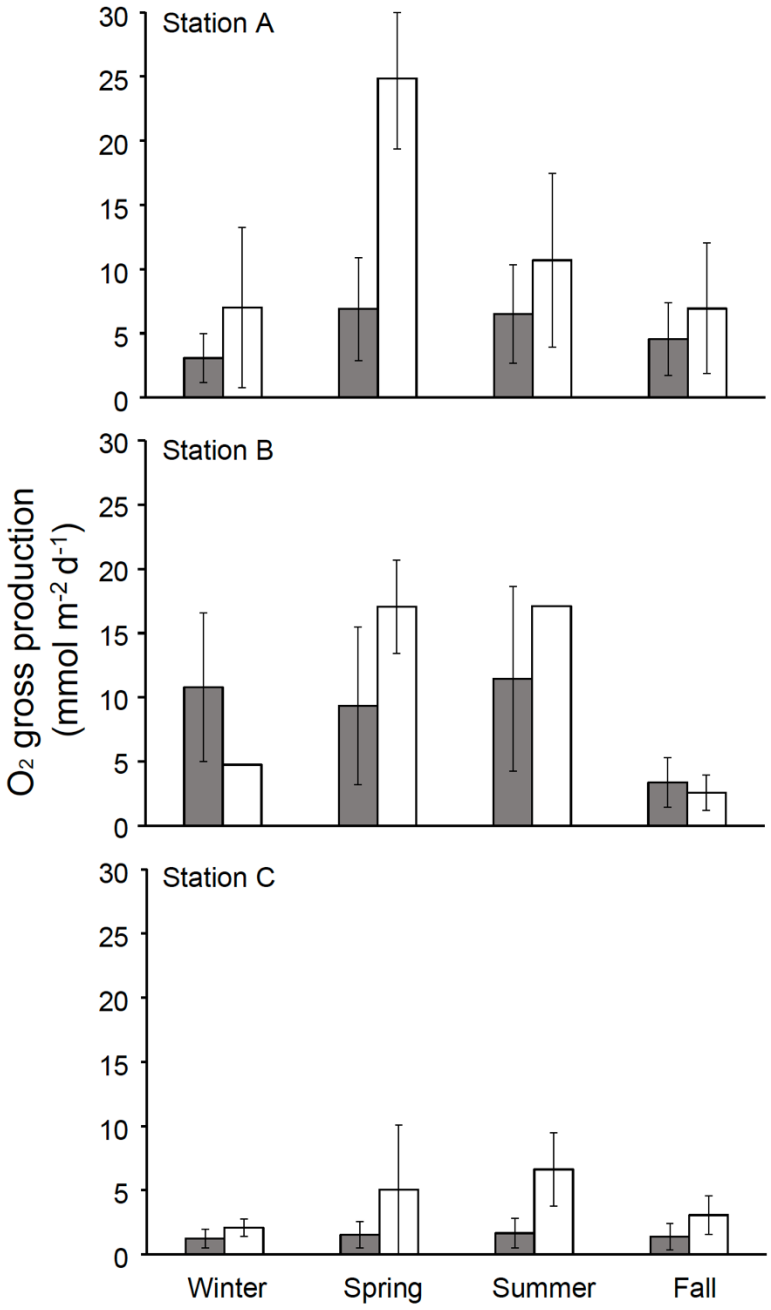

Figure 10: Average gross production at Stations A, B and C determined with in-situ light data and community light response curves (dark grey columns) compared to the average gross production rates determined with an illumination of sediment cores at a light intensity of 200 µE m^{-2} s^{-1} (white columns)

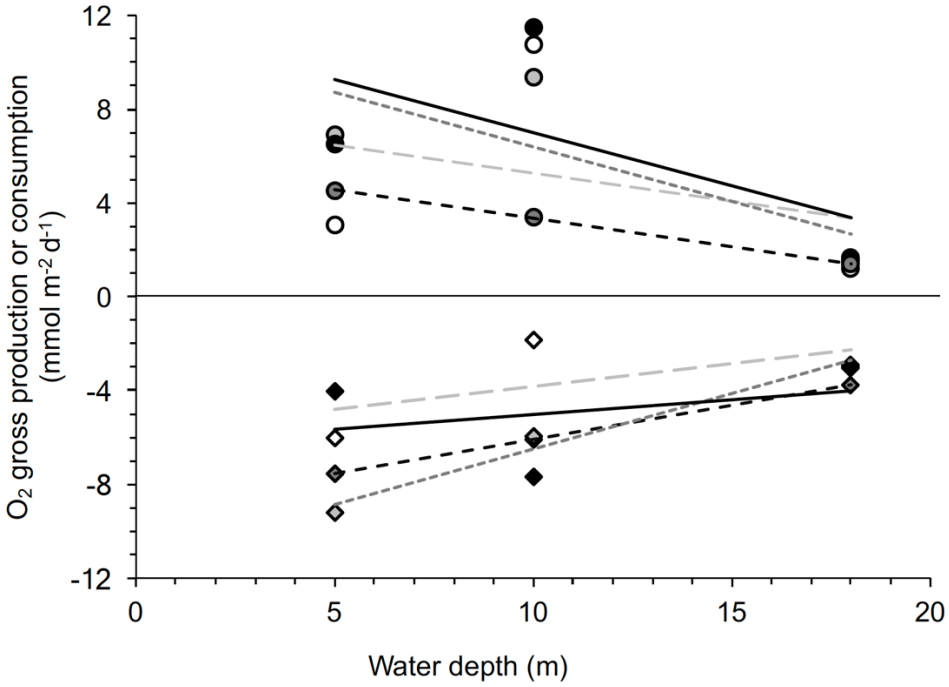

Figure 11. Decrease of gross production (based on in-situ light intensities and community light response curves) and consumption (based on laboratory core incubations) with water depth. Circles: Production, Rhombi: Consumption. White symbols, grey dashed lines: Winter data, light grey, grey dotted lines: spring, black, solid lines: summer, dark grey, black dashed lines: fall.

Table 3: Average daily gross productivities, consumption rates and net productivities calculated based on 1) in-situ PAR measurements and community light response curves, 2) illumination at 200 µE m^{-2} s^{-1}, and the average of calculations 1) and 2). Rates are listed as oxygen (left side of table) and carbon (right side of table) equivalents.

	Gross Prod.		Cons.		Net Prod.		Gross Prod.		Cons.		Net Prod.	
Based on:	AV	SD	AV	SD	AV	SD	AV	SD	AV	SD	AV	SD
200 PAR	(mmol O_2 m^{-2} d^{-1})						(mg C m^{-2} d^{-1})					
A	12.4	11.9	-6.7	3.9	5.7	12.5	114	109	-62	36	52	115
B	10.4	3.9	-5.4	6.0	5.0	7.2	96	36	-50	55	46	66
C	4.2	6.0	-3.2	5.0	1.0	7.8	39	56	-29	46	10	72
In-situ PAR												
A	5.3	6.5	-6.7	3.9	-1.4	7.6	48	60	-62	36	-13	70
B	8.7	11.2	-5.4	6.0	3.3	12.7	81	104	-50	55	31	118
C	1.5	2.0	-3.2	5.0	-1.7	5.4	13	18	-29	46	-16	49

441 3.3. Principle Component Analysis

442 From the distribution of the Eigen values, a natural break was found after the first 2
443 components, which accounted for 50.8% of the variance of all components. The components
444 used modeled the multipliers shown in Table 4.

445

446 **Table 4.** Loading values for each standardized environmental variable for the top two
447 components of the PCA performed in this study.
448

	Component 1	Component 2
Temperature	0.476	-0.282
Salinity	0.275	0.458
Log (Chl *a*)	-0.122	-0.516
Surface PAR	0.145	-0.057
O_2	-0.045	0.435
Log (River discharge)	-0.494	0.054

449

450 There is wide overlap between sites and high and low sediment production dates (Fig.
451 12). This is even more evident when the mean scores for each category are presented with
452 overlapping standard deviation whiskers. For two dates at Station B, and one date at Station C,
453 there was not sufficient continuous data to produce a score from the PCA. Lower O_2 production
454 at Stations A and B was associated with higher temperatures in the bottom water, while higher
455 O_2 production at Station B and A was associated with higher river discharge. Enhanced benthic
456 O_2 production at Station A was related to higher Chl *a* concentrations in the bottom water and
457 river discharge.

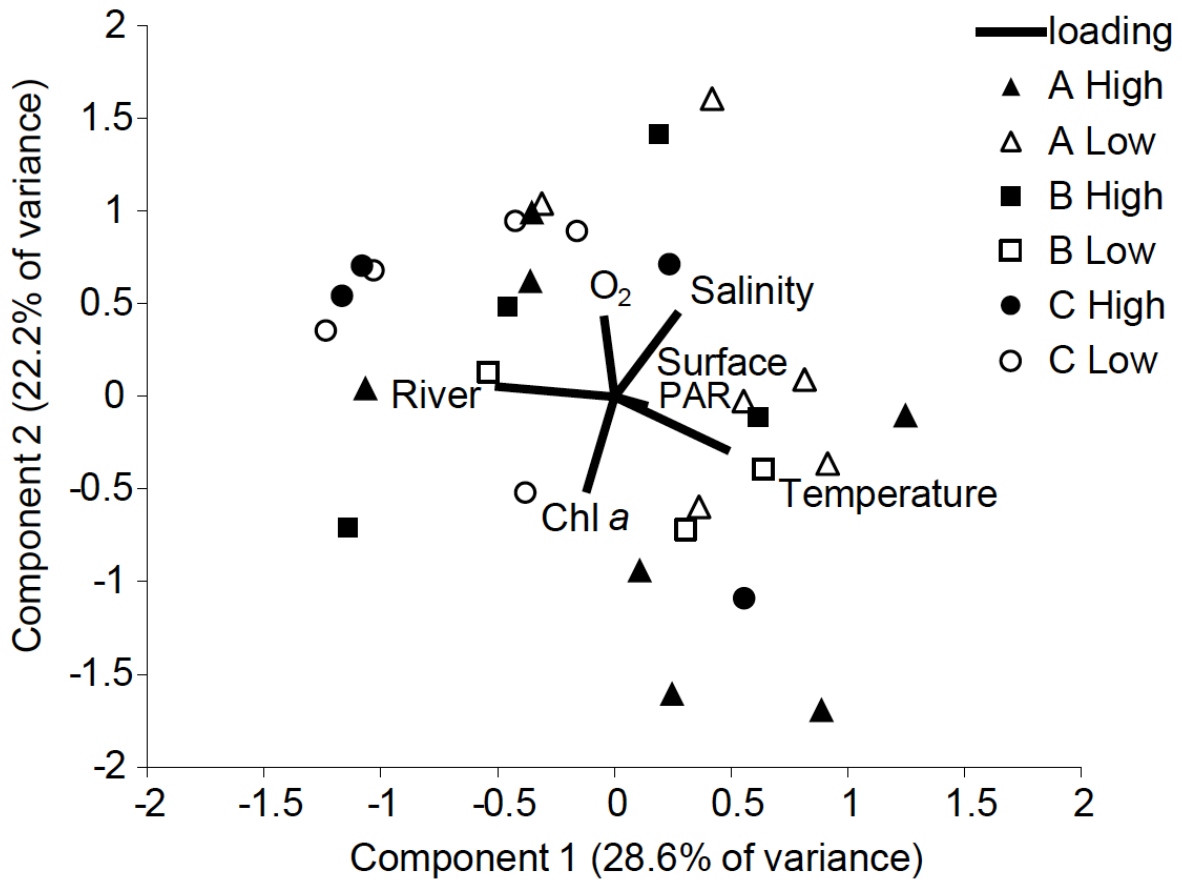

458

459 **Figure 12.** PCA biplot showing the loading of modeled environmental variables (Table 4), and
460 scores of the dates corresponding to sediment O_2 production measurements. For each site, O_2
461 production is divided in half into high and low production.

462

463 **4. Discussion**

464 Very few measurements of benthic photosynthetic production exist for the broad shallow
465 inner shelf of the northeastern Gulf of Mexico (Allison et al., 2013; Berg and Huettel, 2008;
466 Chipman et al., 2016), limiting the understanding of the magnitude and dynamics of this
467 production and its relative contribution to the carbon cycling in the shelf. The time series
468 measurements in this study reveal the changes of the benthic photosynthesis with increasing

469 water depth and between seasons, and the significance of this production for the Big Bend area
470 in the West Florida Shelf. The sandy sediment dominating this area is photosynthetically active
471 over the investigated depth range owing to the microphytobenthos that consisted mainly of
472 pennate diatoms and cyanobacteria as also observed in the sandy inner shelf west of the study
473 transect (Grippo et al., 2009; Grippo et al., 2010). Except winter, spring and summer productivity
474 at B, Benthic gross primary production and sedimentary respiration decreased with increasing
475 water depth, which can be attributed to the coastal gradient of light and nutrients (Santema et al.,
476 2015). The benthic activity followed a seasonal cycle, with highest gross production rates in
477 spring and summer and lowest rates in fall and winter. The spatial and temporal gradients
478 suggest that light availability is the primary factor controlling microphytobenthos productivity
479 because its photosynthetic activity decreased in fall despite temperatures remaining high into the
480 fall and an increase of nutrient availability during winter (Morey et al., 2009; Santema et al.,
481 2015).
482
483 4.1. Light
484 The percent of surface light that reached the sediment surface (0.1 – 29.9%) was
485 comparable to that (0.3 – 16.4%) reported by Grippo et al. (2010) for a sandy area at similar
486 depth (5 – 17 m) in the north-central Gulf of Mexico shelf, and followed the expected trend of
487 decreasing light availability at the seafloor with increasing water depth (Jerlov, 1976).
488 Exceptions from this trend were lower mean and median light fluxes at the nearshore Station A
489 compared to Station C in winter (Fig. 3) that we attribute to increased coastal runoff and
490 sediment resuspension associated with winter storms (Lawson et al., 2007). In winter, adverse
491 weather conditions limited the data that could be retrieved from Station B. The winter data for

492 light at Station B were from a short calm period with clear water. As such, the winter values
493 presented for Station B in Fig. 3 likely are not representative, which can explain why they don't
494 follow the general trend of decreased light availability with increasing water depth. In Table5,
495 the gross O_2 productivity rates we measured for different light intensities are listed with rates
496 reported in the literature. For moderate (~100 μE m^{-2} s^{-1}) and high light intensities (~500 μE m^{-2}
497 s^{-1}), oxygen production rates of the microphytobenthic community sampled at our transect
498 stations were within the same ranges as those measured in the nearby St. Andrews Bay, Panama
499 City, FL, by Murrell et al. (2009b) and the rates reported by Jahnke et al. (2000) for South
500 Atlantic Bight inner shelf sands.

501 **Table 5.** Comparison of CLR values to P-I curve values from the literature. 3 different light
502 intensities are compared, and the range of productivity rates are given.

Source	Date	Location	depth (m)	GPP (mmol O_2 m^{-2} h^{-1})		
				~100 μE m^{-2} s^{-1}	~500 μE m^{-2} s^{-1}	~1000 μE m^{-2} s^{-1}
Murrell, 2009	Summers 2003, 2004	Pensacola Bay, FL	1.5-4.5	-0.4 to 0.8	-0.4 to 3	-
Denis, 2009*	Apr and May 2007	Canche Estuary mudflat, France	intertidal	0.0 to 0.8	0.8 to 6.7	1 to 12.5
Hargrave, 1983	May 1977 to Oct 1980	Bay of Fundy, Canada	intertidal	0.3 to 6.3	0.8 to 16	1.5 to 14.1
Cebrian, 2009 *	Aug to Oct 2003	Perdido Key, FL	shallow, n/a		1.7	2.1
Stutes, 2006 *	Oct 2002 to Jul 2003	Weeks Bay, AL	0.1-1.2	0.2-1.2	1.2 -1.8	
MacIntyre, 1995 * **	Jun-86	Port Aransas, TX	0.4	0.7-4.5	1.2-9	1.3-10.5
MacIntyre, 1996 * **	Mar, Jun, and Jul 1987	San Antonio Bay, TX	1-2.5	0.1	0.2-0.3	0.2-0.4
Jahnke, 2008 *	1999-2005	South Atlantic Bight, GA	27	0.3 to 0.8	1.4 to 3.5	5.7 to 6.9
this study	Jul 2011	Station A	5	0.2 to 0.9	1.4 to 1.9	1.7 to 2.0
this study	Jul 2011	Station B	10	-0.3 to 1.1	1.1 to 4.3	3.1 to 3.2
this study	Jul 2011	Station C	18	-0.3 to 0.3	0.4 to 0.7	0.7 to 0.8
* Originally reported as C production. Assumes a PQ of 1						
** Originally reported as fraction of Chl *a* concentration. Average Chl *a* concentration used for the listed estimate.						

503

504 4.2. Chlorophyll *a*

505 The Chl a concentrations measured along our transect were similar to concentrations
506 reported from sandy shelf sediments of Onslow Bay, North Carolina (Cahoon et al., 1990), the
507 South Atlantic Bight (Jahnke et al., 2008; Nelson et al., 1999) and the Georgia Bight (Hanson et
508 al., 1981). Three to six times higher microphytobenthos Chl *a* concentrations were reported from

509 nearby sandy sediments at similar depths off the coast of Louisiana, which can be explained by
510 the nutrient input of the Mississippi River that affects that area (Grippo et al., 2009; Grippo et al.,
511 2010). Although our transect was reached by the plume of the Apalachicola River, nutrient
512 concentrations in this area are typically low (Table 1, Santema et al.(2015)), and nutrient
513 depletion may explain the low benthic Chl *a* concentrations recorded at stations B and C during
514 summer month (Fig. 4). In contrast, mean Chl *a* concentrations at Station A were highest during
515 summer. Suryaputra et al. (2015) showed that in this region, groundwater discharge within the
516 nearshore zone reaches maximum rates in the summer. Nutrient release with the groundwater
517 (Santos et al., 2009) thus may have contributed to the increased Chl *a* concentration at the
518 nearshore station A during summer. The presence of seagrass beds within 5 km of Sites A and B
519 may have contributed Chl *a* through burial of seagrass debris, but visible pieces of seagrass only
520 rarely were observed in the sediment cores, and we consider this Chl *a* source as minor in our
521 samples.
522 At the shallow station A, frequent movement and resuspension of the sand led to
523 sediment winnowing, mechanical stress and burial of microphytobenthos (Jahnke et al., 2008;
524 MacIntyre and Cullen, 1995; Santema et al., 2015) especially during winter and spring when
525 winds and waves reach maximum strengths (Weisberg et al., 2005). This is supported by winter
526 and spring Chl *a* profiles that, in contrast to the profiles recorded at stations B and C, increased
527 below the surface to reach maximum concentration at approximately 5 cm depth. Such a
528 reduction of Chl *a* in the surface layer of shallow sand beds and a subsurface Chl *a* maximum are
529 common in nearshore sands (e.g. Cartaxana, Mendes et al. (2006), Jesus, Brotas et al. (2009)).
530 Our time series revealed a drop in surface layer Chl *a* concentration between June and September
531 2009. In August 2009, tropical Storm Claudette formed over the West Florida Shelf with winds

that attained 95 km h^{-1}, moved over our study area, and then made landfall about 100 km west. The substantial sediment resuspension and redeposition associated with this storm can explain the observed drop and prolonged depression of the Chl *a* concentration after this event.

4.3. Benthic production rate estimates.

All benthic production and consumption rates presented in this study rely on laboratory measurements (measured in core incubations at a defined light intensity or calculated from community light response curves determined from sediment incubations as different light intensities applied to in-situ light records) and therefore may include errors caused by e.g. inadequate representation of bottom currents or nutrient supply. In-situ chamber measurements of benthic activity face similar problems as these incubations also influence the bottom currents and light (Allison et al., 2013; Jahnke et al., 2008). Chipman et al. (2016) used the eddy covariance method (Berg et al., 2003) for oxygen flux measurements in the sublittoral zone (water depth ~2 m) near Apalachicola/Florida and reported fluxes that are one to two orders of magnitude higher than those found in our study. Benthic production and consumption may increase exponentially with decreasing water depth due to the non-linear attenuation of light in seawater and the reduced dilution of terrigenous nutrients in the nearshore zone (Huettel et al., 2014a; Middelburg and Soetaert, 2004; Middelburg et al., 1997). The sites studied by Chipman et al. (2016) are also very close to the mouth of the Apalachicola River and are affected more strongly by the nutrient discharge of the river.

555 4.4. Potential Production Rates

556 The measurements of the oxygen production at the same light intensity in sediment cores
557 retrieved from the three stations permitted a comparison of the potential production rates
558 between stations and seasons. Although the 200 μE m^{-2} s^{-1} light intensity used for these
559 measurements was also recorded in-situ at each of the three stations during days with low
560 turbidity (Table 1), this light intensity was above the average light intensities reached at each
561 station during the year (A: 107 ± 84 μE m^{-2} s^{-1}, B: 99 ± 82 μE m^{-2} s^{-1}, C: 76 ± 60 μE m^{-2} s^{-1}) and
562 the measured production rates are considered near-maximum rates. The ranges of benthic gross
563 oxygen production and consumption thus may span 1.0 to -0.6 mmol m^{-2} h^{-1} at Station A, 0.8 to -
564 0.5 mmol m^{-2} h^{-1} at B, and 0.3 to -0.3 mmol m^{-2} h^{-1} at C. The general decrease of production and
565 consumption with increasing water depth (Figs. 10, 11) can be explained by the higher
566 concentrations of nutrient and light in the shallow nearshore, which may result in a denser
567 microphytobenthos colonization of the sands as reflected also by the higher Chl *a* concentrations
568 recorded at Station A and B (4 and 13 km from coast, 5 and 10 m deep) compared to Station C
569 (29 km from coast, 18 m deep). The summer values measured for Station B sediments did not
570 follow the trends of decreasing activity with increasing depth but this exception is supported by
571 the independent gross productivity calculations based on the community light response curves.
572 The relatively higher benthic production and consumption rates at B may be linked to a slightly
573 more sheltered position of this station as indicated by the isobaths (Fig. 1), which may have
574 reduced surface sediment mixing and thereby promoted microphytobenthos activities.

575 4.5. Benthic production based on community light response curves

576 The community light response curves we determined agree with community light
577 response curves reported in the literature. In Table 5, the gross O_2 productivity rates we

578 measured for different light intensities are listed with rates reported for comparable sedimentary
579 environments. For moderate (~100 µE m^{-2} s^{-1}) and high light intensities (~500 µE m^{-2} s^{-1}),
580 oxygen production rates of the microphytobenthic community sampled at our transect stations
581 were within the same ranges as those measured in the nearby St. Andrews Bay, Panama City, FL,
582 by Murrell et al. (2009b) and the rates reported by Jahnke et al. (2000) for South Atlantic Bight
583 inner shelf sands.

584 **Table 5.** Comparison of CLR values to P-I curve values from the literature. 3 different light
585 intensities are compared, and the range of productivity rates are given.

Source	Date	Location	depth (m)	GPP (mmol O_2 m^{-2} h^{-1})		
				~100 µE m^{-2} s^{-1}	~500 µE m^{-2} s^{-1}	~1000 µE m^{-2} s^{-1}
Murrell, 2009	Summers 2003, 2004	Pensacola Bay, FL	1.5-4.5	-0.4 to 0.8	-0.4 to 3	-
Denis, 2009*	Apr and May 2007	Canche Estuary mudflat, France	intertidal	0.0 to 0.8	0.8 to 6.7	1 to 12.5
Hargrave, 1983	May 1977 to Oct 1980	Bay of Fundy, Canada	intertidal	0.3 to 6.3	0.8 to 16	1.5 to 14.1
Cebrian, 2009 *	Aug to Oct 2003	Perdido Key, FL	shallow, n/a		1.7	2.1
Stutes, 2006 *	Oct 2002 to Jul 2003	Weeks Bay, AL	0.1-1.2	0.2-1.2	1.2 -1.8	
MacIntyre, 1995 * **	Jun-86	Port Aransas, TX	0.4	0.7-4.5	1.2-9	1.3-10.5
MacIntyre, 1996 * **	Mar, Jun, and Jul 1987	San Antonio Bay, TX	1-2.5	0.1	0.2-0.3	0.2-0.4
Jahnke, 2008 *	1999-2005	South Atlantic Bight, GA	27	0.3 to 0.8	1.4 to 3.5	5.7 to 6.9
this study	Jul 2011	Station A	5	0.2 to 0.9	1.4 to 1.9	1.7 to 2.0
this study	Jul 2011	Station B	10	-0.3 to 1.1	1.1 to 4.3	3.1 to 3.2
this study	Jul 2011	Station C	18	-0.3 to 0.3	0.4 to 0.7	0.7 to 0.8
* Originally reported as C production. Assumes a PQ of 1						
** Originally reported as fraction of Chl *a* concentration. Average Chl *a* concentration used for the listed estimate.						

586

587 Benthic gross oxygen production calculated using the community light response curves
588 and in-situ light intensities in general were lower than the rates calculated from the core
589 incubation at 200 µE m^{-2} s^{-1} light intensity because the average daily peak in-situ light intensities
590 were approximately 2 (Stations A, B) to 2.6 (C) times lower. For the light intensity of 200 µE
591 m^{-2} s^{-1}, the community light response curves produced gross oxygen production values that for
592 Station A and B sediments were similar to those calculated from the core incubations at 200 µE
593 m^{-2} s^{-1}, which were done throughout the study period independently from the community light
594 response curves. This suggests that the community light response curves can produce realistic

595 production data when used with in-situ light intensities. The ranges of benthic gross production
596 rates we determined with the in-situ light intensities and the community light response curves
597 (Station A: 0.4 ± 0.1 mmol m^{-2} h^{-1}, B: 0.7 ± 0.3 mmol m^{-2} h^{-1}, C: 0.1 ± 0.1 mmol m^{-2} h^{-1}) are
598 similar to those recorded in nearby coastal sediments of Pensacola Bay/Gulf of Mexico (Murrell
599 et al., 2009a)) and Galveston Bay/Gulf of Mexico (An and Joye, 2001), as well as ranges
600 reported from marine sediments of similar depths in the South Atlantic Bight and Ngamahau Bay
601 (New Zealand) (Table 6). Our gross production rates were about factor 5 less than those
602 measured by Allison et al. (2013) at 16 m water depth near Pensacola Beach/Gulf of Mexico,
603 located approximately 300 km west of our transect. The 2 to 6 times higher DIN concentrations
604 reported by these authors suggest that their study site received more nutrients than the benthos at
605 our stations, resulting in 20-40 times higher Chlorophyll *a* concentrations and the higher gross
606 primary production rates.
607 The temporal changes of gross oxygen production and respiration along our transect in
608 general followed a seasonal cycle typical for temperate environments, where increases of light
609 and temperature in spring lead to a phytobenthos bloom that benefits from increased water
610 nutrient concentrations resulting from the reduced phytoplankton activity during the winter
611 (Chatterjee et al., 2013). The decrease in microphytobenthos productivity in fall is attributed to
612 the decrease in light and competition for nutrients (Chatterjee et al., 2013) and shading by the
613 relatively high phytoplankton concentrations that can be reached in this area in fall (Santema et
614 al., 2015).
615
616
617

Table 6. Primary production, respiration rates and Chlorophyll *a* concentrations of shallow sandy sediment from different locations as reported in the literature.

Source	Date	Location	Water Depth	GPP	SD	Res	SD	NPP	SD	Chl *a*
			(m)	mmol O_2 m^{-2} h^{-1}						(mg m^{-2})
Hancke & Glud 2004	2-Mar	Trondheimsfjord/Norway	3	10		-10		0		24
Gillespie et al. 2000	Feb-93	Ngamahau Bay, New Zealand	6 - 8	1.1	1.2	-1.3	0.9	-0.2	1.2	
	Feb-93	Ngamahau Bay, New Zealand	19 - 20	2.2	1.3	-0.7	0.4	1.5	1.1	
	Apr-93	Ngamahau Bay, New Zealand	6 - 8	1.3	0.9	-0.4	0.3	0.9	1.2	24
	Apr-93	Ngamahau Bay, New Zealand	15 - 16	0.8	1.1	-0.2	0.1	0.6	1.1	12
	Apr-93	Ngamahau Bay, New Zealand	19 - 20	1.1	1.2	-1.3	0.9	-0.2	1.2	6
	Sep-93	Ngamahau Bay, New Zealand	6 - 8	1.1	0.5	-0.4	0.1	0.7	0.3	25
	Sep-93	Ngamahau Bay, New Zealand	15 - 16	0.1	0.2	-0.3		-0.2		25
	Sep-93	Ngamahau Bay, New Zealand	19 - 20	0.2	0.2	-0.3		-0.1	0.2	12
	Feb-94	Ngamahau Bay, New Zealand	6 - 8	0.9	1	-1	1.1	-0.1	0.1	160
	Feb-94	Ngamahau Bay, New Zealand	15 - 16	1.1	0.3	-0.8	0.3	0.3	0.3	70
	Feb-94	Ngamahau Bay, New Zealand	19 - 20	0.3	0.2	-0.4	0.3	-0.1	0.1	50
Cibic et al. 2008	3-Jul	Gulf of Trieste	17					2.9	0.6	
	3-Dec	Gulf of Trieste	17					-0.6	0.3	
Denis et al. 2009*	7-Apr	Canche Estuary, France	Intertidal	12.1		-1.8	0.7	10.3	0.7	44 µg g^{-1}
	7-Apr	Canche Estuary, France	Intertidal	2.3						34 µg g^{-1}
	7-May	Canche Estuary, France	Intertidal	0.7						13 µg g^{-1}
Bartoli et al. 2003	Sep-98	Tjarno, Sweden (brackish pond)	0.2	4.4	0.4	-10.9	0.3	-6.5	0.5	
Sundback et al. 2011*	7-Jun	Baltic Sea, Sweden	0.3	1.7						
Sundback et al. 1988	Jul-87	Stromstad, Sweden	0.2					4.4		
Webster et al. 2002	Dec-97	Lake Illawarra, Australia (brackish lagoon)	1	14.8						
	Dec-97	Lake Illawarra, Australia (brackish lagoon)	10	18.1						
Jahnke et al. 2000*	May-96	South Atlantic Bight	27	0.7	0.1	-0.1	0.4	0.6	0.4	20.8
	May-96	South Atlantic Bight	30	0.8	0.1	-1.3	0.3	-0.5	0.3	21.6
	May-96	South Atlantic Bight	27	1.4	0.1	-0.9	0.1	0.4	0.1	20.8
	May-96	South Atlantic Bight	27	1.3	0.1	-1	0.1	0.3	0.1	20.8
	Aug-96	South Atlantic Bight	27	2.2	0.1	-1.5	0.1	0.6	0.2	20.8
	Aug-96	South Atlantic Bight	35	0.7	0.2	-1	0	-0.3	0.2	21.6
	Aug-96	South Atlantic Bight	14	2.9	0.1	-3	0.1	-0.1	0.2	28.7
	Aug-96	South Atlantic Bight	40	0.5	0.2	-1	0.2	-0.5	0.2	11.2
	Aug-96	South Atlantic Bight	27	2.6	0.1	3.6	0.2	-1	0.2	20.8
	Sep-96	South Atlantic Bight	14	2.1	0.1	1.7	0.1	0.5	0.1	28.7
	Sep-96	South Atlantic Bight	27	0.2	0.1	0.9	0.1	-0.7	0.1	20.8
Burton Evans 2005	Jan-Aug 04	Florida Bay	1	5.7	1.1	-4.1	5.1	1.6	5.2	30.2
	Jan-04	Florida Bay	1	8.9	1.5	-2.3	0.3	6.6	1.5	
	Mar-04	Florida Bay	1	10.9	0.7	-2.8	0.2	8.1	0.7	
	Jun-04	Florida Bay	1	12.4	0.9	-5	0.4	7.4	1	
	Aug-04	Florida Bay	1	5.4	0.3	-3.4	0.3	2	0.4	
An et al. 2001	Jan-97	Galveston Bay TX	4	1.5		-1.2		0.3		
	Aug-97		4	0.3		-1.9		-1.6		
Murrell et al. 2009	Summers 03, 04	Shoals Pensacola Bay , FL	1.5	1.1	1	-1.4	0.8	-0.3	1.3	206.4
	Summers 03, 04	Channel, Pensacola Bay , FL	4.5	0.1	0.1	-0.9	0.7	-0.8	0.7	96
Allison et al. 2013	4-Sep	Pensacola Bay, FL	15	4.3		-2.9		1.4		
	4-Sep	Pensacola Bay, FL	15	5.5		-2.7		2.8		
	4-Sep	Pensacola Bay, FL	15	4.8		-3.3		1.5		4.8 µg g^{-1}
	4-Sep	Pensacola Bay, FL	16	4.5		-3.7		0.8		
	5-Jul	Pensacola Bay, FL	15	2.5		-1.3		1.2		
	5-Jul	Pensacola Bay, FL	15	2.1		-1.3		0.8		
this study	Sep 08 to Sep 10	Station A	5	0.4	0.5	-0.6	0.3	-0.1	0.6	0.2 µg g^{-1}
	Sep 08 to Jun 10	Station B	10	0.7	0.9	-0.5	0.5	0.2	1.0	0.2
	Sep 08 to Jun 10	Station C	18	0.1	0.2	-0.3	0.4	-0.1	0.4	0.1

*Originally reported in C production. Assumes a PQ of 1.

622 4.6. Principal Component Analysis (PCA)

623 The Principal Component Analysis provided insights on the response of the benthic
624 production to some key environmental factors. The inverse relationship between temperature and
625 river discharge in Component 1 (Fig. 12) reflects seasonal trends and the response of temperature
626 to stormier conditions. The association of lower O_2 production rates at Stations A and B with
627 higher temperatures in the bottom water thus may indicate the effects of nutrient depletion during
628 calm periods with reduced water exchange, while the association of higher O_2 production rates at
629 Station B and A with and river discharge suggest the effect of increased nutrient concentrations
630 caused by riverine input. Likewise, higher O_2 production rates at Station A, the station closest to
631 the shore, were related to river discharge and Chl *a* in the bottom water, pointing to direct and
632 indirect effects of enhanced nutrient supply. The inverse relationship of bottom water Chl *a* to
633 both salinity and bottom water oxygen in Component 2 could be a consequence of upwelling of
634 deeper, more saline, water (Santema et al., 2015) or increased decay when more algal organic
635 matter is in the water column. The positioning of the low O_2 production rates of station C within
636 the PCA diagram suggests that this, the deepest station, was perhaps most impacted by light
637 availability, with surface PAR and temperature (more light in warmer seasons) closely related in
638 Component 2.

639

640 4.7. Balance of production and consumption

641 The general trend of highest gross production and respiration rates at the shallower
642 stations and lowest rates at the deepest station (Figs. 7, 11) reflect the effect of the coastal energy
643 gradient, where the input of nutrients and organic matter from land, light penetration to the
644 bottom and intensity of water column mixing all peak in the shallow inner shelf (Denis and

Desreumaux, 2009; Huettel et al., 2014b; Webster et al., 2002). Our core incubations using 200 µE m^{-2} s^{-1} light intensity produced production rates near the maximum, while the community light response curves may underestimate production rates because the incubations excluded nutrient and CO_2 supply from deeper sediment layers (Cook and Roy, 2006) and were conducted at low nutrient concentrations to limit microphytobenthos growth during the experiment. Nevertheless, the ranges of the production rates calculated with the two approaches were not far apart (Fig. 10), suggesting that the in-situ rates may range among the lower and upper limits produced by these two approaches (Fig. 13). The regression of the average net benthic production rates determined from community light response curves/in-situ light, and average consumption rates from core incubations suggest that production and consumption were balanced along our transect. During clear water periods allowing high light intensities at the bottom as observed at Station B during winter (Fig. 3), temporary autotrophic conditions may reach down to ~20 m (Fig. 13). Since respiration rates generally scaled with production rates, the sedimentary heterotrophic metabolism may be closely linked to the respiration of photosynthetic products. Highest consumption rates were recorded in spring for Station A. Water temperatures did not drop below 11°C and thus did not substantially impede heterotrophic activity. The increased abundance of microphytobenthos in spring also increased the respiration during darkness, and its growth thus may have fueled heterotrophic metabolism, e.g. that of microbes consuming diatom exudates and grazers (Middelburg et al., 2000).

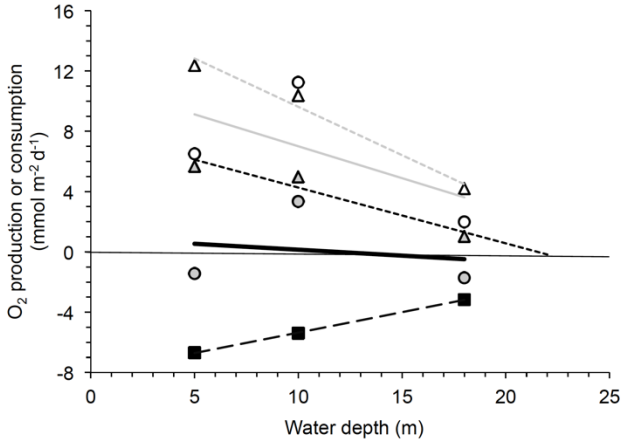

Figure 13. Depth limits of average net benthic productivity. The regression (thick black solid line) of net production rates (grey circles) determined from community light response curves/in-situ light (white circles, solid grey regression line) and average consumption rates from core incubations (black squares, black dashed regression line) suggest that the benthic system along our transect is balanced. Black dotted line: regression of maximum net production rates (grey triangles) determined from core incubations at a light intensity of 200 µE m^{-2} s^{-1} (white triangles, grey dotted regression line) and average consumption rates from core incubations (black squares, black dashed regression line).

5. Conclusions

The results of the two independent approaches used to determine benthic primary production rates along the study transect agreed relatively well, supporting that average sediment gross primary production rates in this area of the West Florida Shelf increase from ~15 mg C m^{-2} d^{-1} at ~20 m water depth to ~80 mg C m^{-2} d^{-1} at 10 m water depth. Santema et al. (2015) measured water column production rates of 53 to 106 mmol C m^{-2} d^{-1} along this transect in July 2009, implying that the benthic production here may contribute up to 50% to the shelf production.

Acknowledgments

We thank Sonja Bridges from the FSU Marine and Coastal Laboratory Academic Diving Program, and our boat captains Roseanne Weglinski and Mike Lavendar. Eric Howarth and Stephanie White helped with the maintenance and deployment of the YSI multi-probes. Funding: This research was supported by NOAA (NGI grant 023320), NSF (OCE-424967, OCE-536431, and OCE-726754), and the Geophysical Fluid Dynamics Institute at FSU.

References

Allesson, L., Strom, L., Berggren, M., 2016. Impact of photochemical processing of DOC on the bacterioplankton respiratory quotient in aquatic ecosystems. Geophysical Research Letters 43, 7538-7545.

Allison, J.G., Wagner, M.E., McAllister, M., Ren, A.K.J., Snyder, R.A., 2013. Sand bottom microalgal production and benthic nutrient fluxes on the northeastern gulf of mexico nearshore shelf. Gulf and Caribbean Research 25, 1-8.

An, S., Joye, S.B., 2001. Enhancement of coupled nitrification–denitrification by benthic photosynthesis in shallow estuarine sediments. Limnol. Oceanogr. 46, 62–74.

Bartoli, M., Nizzoli, D., Viaroli, P., 2003. Microphytobenthos activity and fluxes at the sediment-water interface: interactions and spatial variability. Aquatic Ecology 37, 341-349.

Baustian, M.M., Rabalais, N.N., Morrison, W.L., Turner, R.E., 2011. Seasonal microphytobenthos on the hypoxic northern Gulf of Mexico continental shelf. Marine Ecology Progress Series 436, 51-66.

Berg, P., Huettel, M., 2008. Monitoring the Seafloor Using the Noninvasive Eddy Correlation Technique: Integrated Benthic Exchange Dynamics. Oceanography 21, 164-167.

Berg, P., Roy, H., Janssen, F., Meyer, V., Jorgensen, B.B., Huettel, M., de Beer, D., 2003. Oxygen uptake by aquatic sediments measured with a novel non-invasive eddy-correlation technique. Marine Ecology-Progress Series 261, 75-83.

Burton Evans, J.L., 2005. The effect of benthic microalgal photosynthetic oxygen production on nitrogen fluxes across the sediment-water interface in a shallow, sub-tropical estuary. MSc thesis. University of Maryland, Annapolis, MD.

713 Cahoon, L., 1999. The role of benthic microalgae in neritic systems. Oceanography and Marine
714 Biology: an Annual Review 37, 47-86.
715 Cahoon, L.B., Redman, R.S., Tronzo, C.R., 1990. Benthic Microalgal Biomass in Sediments of
716 Onslow Bay, North-Carolina. Estuarine Coastal and Shelf Science 31, 805-816.
717 Canfield, D.E., Jørgensen, B.B., Fossing, H., Glud, R., Gundersen, J., Ramsing, N.B., Thamdrup,
718 B., Hansen, J.W., Nielsen, L.P., Hall, P.O.J., 1993. Pathways of organic carbon oxidation in
719 three continental margin sediments. Mar. Geol. 113, 27-40.
720 Cartaxana, P., Mendes, C.R., van Leeuwe, M.A., Brotas, V., 2006. Comparative study on
721 microphytobenthic pigments of muddy and sandy intertidal sediments of the Tagus estuary.
722 Estuarine Coastal and Shelf Science 66, 225-230.
723 Cebrian, J., Corcoran, A.A., Stutes, A.L., Stutes, J.P., Pennock, J.R., 2009. Effects of ultraviolet-
724 B radiation and nutrient enrichment on the productivity of benthic microalgae in shallow
725 coastal lagoons of the North Central Gulf of Mexico. Journal of Experimental Marine
726 Biology and Ecology 372, 9-21.
727 Chatterjee, A., Kleina, C., Naegelena, A., Claquinb, P., Massona, A., Legoff, M., Amicea, E.,
728 L'Helguena, S., Chauvauda, L., Leynaert, A., 2013. Comparative dynamics of pelagic and
729 benthic micro-algae in a coastal ecosystem. Estuarine, Coastal and Shelf Science 133, 67-77.
730 Chipman, L., Berg, P., Huettel, M., 2016. Benthic Oxygen Fluxes Measured by Eddy Covariance
731 in Permeable Gulf of Mexico Shallow-Water Sands. Aquatic Geochemistry 22, 529-554.
732 Chipman, L., Huettel, M., Laschet, M., 2012. Effect of benthic-pelagic coupling on dissolved
733 organic carbon concentrations in permeable sediments and water column in the northeastern
734 Gulf of Mexico. Continental Shelf Research 45, 116-125.

735 Cibic, T., Blasutto, O., Burba, N., Umani, S.F., 2008. Microphytobenthic primary production as
736 C-14 Uptake in sublittoral sediments of the Gulf of Trieste (northern Adriatic Sea):
737 Methodological aspects and data analyses. Estuarine Coastal and Shelf Science 77, 113-122.
738 Colijn, F., de Jonge, V.N., 1984. Primary production of microphytobenthos in the Ems-Dollard
739 Estuary. Marine Ecology 14, 185-196.
740 Cook, P.L.M., Roy, H., 2006. Advective relief of CO2 limitation in microphytobenthos in highly
741 productive sandy sediments. Limnol. Oceanogr. 51, 1594-1601.
742 Denis, L., Desreumaux, P.E., 2009. Short-term variability of intertidal microphytobenthic
743 production using an oxygen microprofiling system. Marine and Freshwater Research 60,
744 712-726.
745 Gattuso, J.P., Gentili, B., Duarte, C.M., Kleypas, J.A., Middelburg, J.J., Antoine, D., 2006. Light
746 availability in the coastal ocean: impact on the distribution of benthic photosynthetic
747 organisms and their contribution to primary production. Biogeosciences 3, 489-513.
748 Gillespie, P.A., Maxwell, P.D., Rhodes, L.L., 2000. Microphytobenthic communities of subtidal
749 locations in New Zealand: taxonomy, biomass, production, and food-web implications. New
750 Zealand Journal of Marine and Freshwater Research 34, 41-53.
751 Grasshoff, K., Klaus Kremling, K., Ehrhardt, M., 1999. Methods of Seawater Analysis, 3rd
752 Edition.
753 Grippo, M., Fleeger, J.W., Condrey, R., Carman, K.R., 2009. High benthic microalgal biomass
754 found on ship shoal, north-central gulf of mexico. Bulletin of Marine Science 84, 237-256.
755 Grippo, M.A., Fleeger, J.W., Rabalais, N.N., Condrey, R., Carman, K.R., 2010. Contribution of
756 phytoplankton and benthic microalgae to inner shelf sediments of the north-central Gulf of
757 Mexico. Continental Shelf Research 30, 456-466.

758 Hancke, K., Glud, R.N., 2004. Temperature effects on respiration and photosynthesis in three
759 diatom-dominated benthic communities. Aquatic Microbial Ecology 37, 265-281.
760 Hanson, R.B., Tenore, K.R., Bishop, S., Chamberlain, C., Pamatmat, M.M., Tietjen, J., 1981.
761 Benthic enrichment in the georgia bight related to gulf-stream intrusions and estuarine
762 outwelling. Journal of Marine Research 39, 417-441.
763 Hargrave, B.T., Prouse, N.J., Phillips, G.A., Neame, P.A., 1983. Primary production and
764 respiration in pelagic and benthic communities at 2 intertidal sites in the upper bay of fundy.
765 Canadian Journal of Fisheries and Aquatic Sciences 40, 229-243.
766 He, R.Y., Weisberg, A.H., 2002. Tides on the West Florida shelf. Journal of Physical
767 Oceanography 32, 3455-3473.
768 Huettel, M., Berg, P., Kostka, J.E., 2014. Benthic Exchange and Biogeochemical Cycling in
769 Permeable Sediments. Annual Review of Marine Science, Vol 6 6, 23-51.
770 Jahnke, R.A., Nelson, J.R., Marinelli, R.L., Eckman, J.E., 2000. Benthic flux of biogenic
771 elements on the Southeastern US continental shelf: influence of pore water advective
772 transport and benthic microalgae. Continental Shelf Research 20, 109-127.
773 Jahnke, R.A., Nelson, J.R., Richards, M.E., Robertson, C.Y., Rao, A.M.F., Jahnke, D.B., 2008.
774 Benthic primary productivity on the Georgia midcontinental shelf: Benthic flux
775 measurements and high-resolution, continuous in situ PAR records. J. Geophys. Res. 113.
776 Jerlov, N.G., 1976. Marine optics. Elsevier.
777 Jesus, B., Brotas, V., Ribeiro, L., Mendes, C.R., Cartaxana, P., Paterson, D.M., 2009.
778 Adaptations of microphytobenthos assemblages to sediment type and tidal position.
779 Continental Shelf Research 29, 1624-1634.

780 Lawson, S.E., Wiberg, P.L., McGlathery, K.J., Fugate, D.C., 2007. Wind-driven sediment
781 suspension controls light availability in a shallow coastal lagoon. Estuaries and Coasts 30,
782 102-112.
783 Livingston, R.J., 1984. The ecology of the Apalachicola Bay system: an estuarine profile. U.S.
784 Fish and Wildlife Service. FWS/OBS 82/05, p. 148.
785 MacIntyre, H.L., Cullen, J.J., 1995. Fine-scale vertical resolution of chlorophyll and
786 photosynthetic parameters in shallow-water benthos. Marine Ecology Progress Series 122,
787 227-237.
788 Macintyre, H.L., Geider, R.J., Miller, D.C., 1996. Microphytobenthos: The ecological role of the
789 "secret garden" of unvegetated, shallow-water marine habitats .1. Distribution, abundance
790 and primary production. Estuaries 19, 186-201.
791 Maksimova, E.V., Clarke, A.J., 2013. Multiyear Subinertial and Seasonal Eulerian Current
792 Observations near the Florida Big Bend Coast. Journal of Physical Oceanography 43, 1691-
793 1709.
794 Middelburg, J.J., Soetaert, K., 2004. The role of sediments in shelf ecosystem dynamics.
795 Geochimica Et Cosmochimica Acta 68, A343-A343.
796 Middelburg, J.J., Soetaert, K., Herman, P.M.J., 1997. Empirical Relationships For Use In Global
797 Diagenetic Models. Deep Sea Research Part I Oceanographic Research Papers 44, 327-344.
798 Middelburg, J.J., Barranguet, C., Boschker, H.T.S., Herman, P.M.J., Moens, T., Heip, C.H.R.,
799 2000. The fate of intertidal microphytobenthos carbon: An in situ C-13-labeling study.
800 Limnology & Oceanography 45, 1224-1234.

801 Miller, D.C., Geider, R.J., Macintyre, H.L., 1996. Microphytobenthos: The ecological role of the
802 "secret garden" of unvegetated, shallow-water marine habitats .2. Role in sediment stability
803 and shallow-water food webs. Estuaries 19, 202-212.
804 Morey, S.L., Dukhovskoy, D.S., Bourassa, M.A., 2009. Connectivity of the Apalachicola River
805 flow variability and the physical and bio-optical oceanic properties of the northern West
806 Florida Shelf. Continental Shelf Research 29, 1264-1275.
807 Mortenson, E., 2013. Physical description and analysis of the variability ofsalinity and oxygen in
808 Apalachicola Bay, Department of Earth, Ocean, and Atmospheric Sciences. Florida State
809 University, Tallahassee, FL, p. 65.
810 Murrell, M.C., Campbell, J.G., Hagy, J.D., Caffrey, J.M., 2009. Effects of irradiance on benthic
811 and water column processes in a Gulf of Mexico estuary: Pensacola Bay, Florida, USA.
812 Estuarine Coastal and Shelf Science 81, 501-512.
813 Nelson, J.R., Eckman, J.E., Robertson, C.Y., Marinelli, R.L., Jahnke, R.A., 1999. Benthic
814 microalgal biomass and irradiance at the sea floor on the continental shelf of the South
815 Atlantic Bight: Spatial and temporal variability and storm effects. Continental Shelf Research
816 19, 477-505.
817 Ní Longphurt, S., Clavier, J., Grall, J., Chauvaud, L., Le Loc'h, F., Le Berre, I., Flye-Sainte-
818 Marie, J., Richard, J., Leynaert, A., 2007. Primary production and spatial distribution of
819 subtidal microphytobenthos in a temperate coastal system, the Bay of Brest, France.
820 Estuarine Coastal and Shelf Science 74, 367-380.
821 NOAA-NCEI, 2017. US Coastal Relief Model.
822 NOAA-NOS, 2015. Seagrasses in the Continental Unites States as of March 2015.

823 Okey, T.A., 2002. Primary producers. , in: Okey, T.A., Mahmoudi, B. (Ed.), An Ecosystem
824 Model of the West Florida Shelf for Use in Fisheries Management and Ecological Research.
825 Volume II. Model Construction. Fish and Wildlife Conservation Commission, Florida
826 Marine Research Institute, St. Petersburg.
827 Okey, T.A., Vargo, G.A., Mackinson, S., Vasconcellos, M., Mahmoudi, B., Meyer, C.A., 2004.
828 Simulating community effects of sea floor shading by plankton blooms over the West Florida
829 Shelf. Ecological Modelling 172, 339-359.
830 Parsons, T.R., Maita, Y., Lalli, C.M., 1984. Plant Pigments, A Manual of Chemical and
831 Biological Methods for Seawater Analysis. Pergamon Press, Oxford, England, p. 173.
832 Platt, T., Gallegos, C.L., Harrison, W.G., 1980. Photoinhibition of photosynthesis in natural
833 assemblages of marine phytoplankton. Journal of Marine Research 38, 687-701.
834 Posey, M.H., Alphin, T.D., Banner, S., Vose, F., Lindberg, W., 1998. Temporal variability,
835 diversity and guild structure of a benthic community in the northeastern Gulf of Mexico.
836 Bulletin of Marine Science 63, 143-155.
837 Santema, M., Clarke, A.J., Speer, K., Huettel, M., 2015. Water column oxygen dynamics within
838 the coastal gradient in the northeastern Gulf of Mexico inner shelf. Continental Shelf
839 Research 104, 104-119.
840 Santos, I.R., Burnett, W.C., Dittmar, T., Suryaputra, I., Chanton, J., 2009. Tidal pumping drives
841 nutrient and dissolved organic matter dynamics in a Gulf of Mexico subterranean estuary.
842 Geochimica Et Cosmochimica Acta 73, 1325-1339.
843 Stutes, J., Cebrian, J., Stutes, A.L., Hunter, A., Corcoran, A.A., 2007. Benthic metabolism across
844 a gradient of anthropogenic impact in three shallow coastal lagoons in NW Florida. Marine
845 Ecology Progress Series 348, 55-70.

Sundback, K., Jonsson, B., 1988. Microphytobenthic productivity and biomass in sublittoral sediments of a stratified bay, southeastern kattegat. Journal of Experimental Marine Biology and Ecology 122, 63-81.

Sundback, K., Lindehoff, E., Graneli, E., 2011. Dissolved organic nitrogen: an important source of nitrogen for the microphytobenthos in sandy sediment. Aquatic Microbial Ecology 63, 89-100.

Suryaputra, I.G.N.A., Santos, I.R., Huettel, M., Burnett, W.C., Dittmar, T., 2015. Non-conservative behavior of fluorescent dissolved organic matter (FDOM) within a subterranean estuary. Continental Shelf Research 110, 183-190.

Walsby, A.E., 1997. Numerical integration of phytoplankton photosynthesis through time and depth in a water column. New Phytology 136, 189-209.

Webster, I.T., Ford, P.W., Hodgson, B., 2002. Microphytobenthos contribution to nutrient-phytoplankton dynamics in a shallow coastal lagoon. Estuaries 25, 540-551.

Weisberg, R., H., , He, R.L., Y. , Virmani, J.I., 2005. West Florida Shelf circulation on synoptic, seasonal, and interannual time scales, Circulation in the Gulf of Mexico: Observations and models. AGU.

Yarbro, L.A., Carlson, P.R., 2013. Seagrass Integrated Mapping and Monitoring Program: Mapping and Monitoring Report No. 1. . Fish and Wildlife Research Institute p. 128.